

Comparison of Numerical and Experimental Results for the Evaluation of the Depollution Effectiveness of Photocatalytic Coverings in Street Canyons

N. Moussiopoulos · Ph. Barmpas · I. Ossanlis · J. Bartzis

Received: 30 August 2006 / Accepted: 19 December 2006 / Published online: 17 July 2007
© Springer Science + Business Media B.V. 2007

Abstract Towards the aim of improving the air quality in the urban environment via the application of innovative TiO₂ based photocatalytic coverings, a field campaign took place within the frame of the EU PICADA project (<http://www.picada-project.com>) to assess the expected depollution efficiency of such materials under realistic conditions. Furthermore, extensive numerical modeling was performed via the application of the RANS CFD code for microscale applications MIMO, in an effort to assess the sensitivity of the developing flow field and the corresponding dispersion mechanism and hence of the depollution efficiency of the PICADA products on a wide range of factors, with most notably the length of the street canyon, the thermal exchange between the heated street canyon walls and the air and the approaching wind direction. For the needs of the PICADA project a new, simple module had to be implemented into MIMO to be able to model the removal of NO_x from a street canyon whose walls have been treated with a photocatalytic product. The model simulation results presented in this paper, show that MIMO is indeed capable of predicting the effectiveness of the photocatalytic products in question. At the same time, they reveal a strong dependence of the developing flow and concentration fields inside the field site street canyon configuration on most of the aforementioned factors with most notably the direction of the approaching wind.

Keywords Photocatalytic coverings · Dispersion · Street canyon length · Thermal exchange · Wind direction · NO_x removal

1 Introduction

The aim of the European Project PICADA (<http://www.picada-project.com>), as *Photocatalytic Innovative Coverings Applications for Depollution Assessment*, is to reduce the cost and increase the performances of the innovative coverings for sheet-like applications to make available affordable, really sustainable products via the development of a range of such novel materials, whose large-scale applications, combined with already existing techniques, may improve the air quality of the urban built environment. Furthermore, during the past two decades extensive research regarding the development of titanium dioxide (TiO₂)-based photocatalytic materials and their applications for environmental purposes has been conducted [8, 17], which revealed the potentially beneficial effects of their use, in the removal of various pollutants from the urban environment. Towards this aim, it was decided that a field experiment campaign be carried out in an artificially constructed street canyon configuration designed to approximate real-life urban street canyons, to evaluate the performance and the depollution potential of a range of photocatalytic TiO₂-based façade covering products, which have been developed by the PICADA consortium.

The flow pattern that usually develops in typical real life, relatively narrow urban street canyons usually lies within the skimming flow regime [18]. Previous numerical studies by Sini et al. (1996) [21] showed that the ventilation of the emitted pollution from a street is strongly dependent on the flow regime, with the skimming flow regime always resulting into higher average concentrations inside the

N. Moussiopoulos (✉) · P. Barmpas · I. Ossanlis
Laboratory of Heat Transfer and Environmental Engineering,
Aristotle University,
P.O. Box 483, 54124 Thessaloniki, Greece
e-mail: moussio@eng.auth.gr

J. Bartzis
NCSR “Demokritos”, Institute of Nuclear Technology—Radiation
Protection, Environmental Research Laboratory,
Athens, Greece

street canyons. Further studies demonstrated that for the skimming flow regime within a street, the flow field is characterised by the formation of a centrally located single vortex [4] or a system of counter rotating vortices [20] depending on the street canyon aspect ratio. In addition, previous wind tunnel and numerical studies [1, 2, 19] demonstrated that for street canyons with small street width to building height ratio ($W/H < 0.5$), under neutrally heated conditions the flow field is characterised by a system of at least two counter-rotating vortices with high average concentrations inside the canyon and with the highest ones at the lowest levels of the street canyon. In view of those findings, it was decided that the field site should consist of three artificially constructed street canyons made up of commercial cargo containers with an aspect ratio of 0.4 under a scale of 1:5 of an assumed street canyon consisting of seven-story buildings (~ 25 m), based on the stacking height of those containers. This particular aspect ratio was chosen because it is small enough to ensure high average concentrations inside the street canyon configuration while at the same time it would allow enough space for the installation of the necessary equipment inside the street canyon of interest.

However, previous wind tunnel and numerical studies [12, 14, 16, 21] have demonstrated that the flow field and the corresponding dispersion mechanism inside a street canyon can be largely affected by the buoyant forces that develop caused by the thermal exchange between the heated building walls and the street canyon air. Furthermore, Crowther and Hassan (2002) [5] showed that both the street canyon length and the approaching wind direction can strongly influence the dispersion of pollutants in urban street canyons. The results from those studies led to the decision to apply the numerical model MIMO to study the effects on the flow and dispersion (and hence on the predicted depollution efficiency of the photocatalytic façade covering materials) in street canyons of (a) the street canyon length, (b) the heat transfer between street canyon walls and street canyon ambient air and (c) the approaching wind direction. The findings from the aforementioned numerical studies would be used to (a) properly design the experimental field site configuration and (b) predict the expected depollution effectiveness of the materials that would be tested.

Overall, the comparison between numerical simulations and experimental results shows that MIMO is capable of describing the impact of photocatalytic coverings on the NO_x levels in an urban street canyon. Furthermore, the results reveal a strong influence of both the street length and the approaching wind direction on the flow field and the pollutant concentration patterns inside the street. Also, although numerical results show a strong dependence of the flow and dispersion on the heat transfer between the building walls and the air, especially inside deep street canyons, it seems that in this specific experiment thermal

effects seem to affect only slightly the overall performance of the photocatalytic materials.

2 The PICADA Field Campaign

The campaign was conducted during the period May–September 2004, as the meteorological conditions in that region during the summer months and particularly July are usually characterised by high solar intensities and low wind speeds. Under low wind conditions, the expected concentration of pollutants released from a line source of emissions within the street canyon in question would be higher compared to the ones expected under the usually higher wind conditions during the rest of the seasons. Furthermore, the heating of the street canyon walls caused by the high solar radiation during the summer months would enable us to study the effects of thermal exchange between the street canyon walls and the air on the flow and concentration fields inside the street canyon.

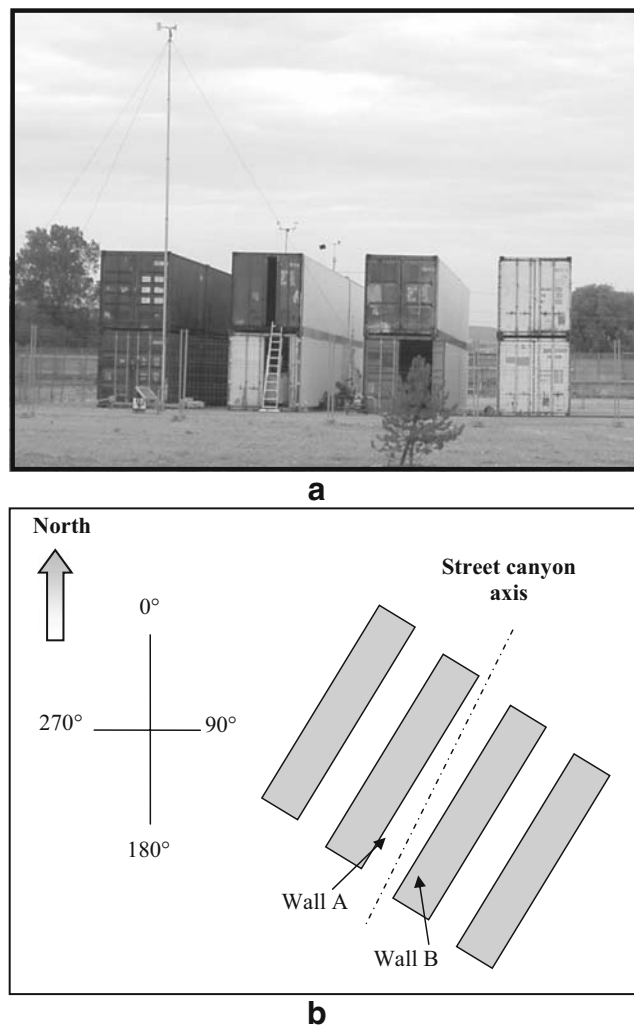


Fig. 1 (a) Side view of the experimental street canyon configuration with the two meteorological stations masts and (b) field site orientation



Fig. 2 Perforated tube used as a line source of emissions inside the 2nd consecutive street canyon

2.1 Description of the Field Site

The field site set up consisted of three artificially constructed consecutive street canyons, made up of commercial cargo containers under a scale of 1:5 of an assumed street canyon with length ~ 100 m and consisting of seven-story buildings (~ 25 m), based on the stacking height of those containers. All three street canyons had the same geometrical characteristics, namely, a street width W of 2 m, a street height H of 5.2 m and a street length L of 18.2 m, with a resulting street width to street height ratio (aspect ratio) W/H of ~ 0.4 and a street width to street length ratio W/L of ~ 0.1 . The field site was located in the industrial area in Guerville, France, which is about 40 km west of Paris, in the valley of Seine. During the period covering the field campaign, the prominent wind direction is usually parallel to the axis of the valley which forms an angle of $\sim 52^\circ$ with respect to the North. As a result, the experimental street canyon configuration was orientated at the same angle with respect to the North as the Seine valley axis, to achieve approach flow wind directions with respect to the street canyon axis of the configuration as close to perpendicular

as possible. During the entire field campaign period, background meteorological measurements of the approaching wind direction WD , of the approaching wind speed WS , of the ambient temperature T , of the relative humidity RH and of the solar irradiation were taken from two different meteorological stations, one at 3 m above the roof level of the second array of containers and one at 5 m above the roof level (10 m above the ground) south of the street canyon configuration. Background NO_x and O_3 concentrations were also continuously recorded above the roof level of the second consecutive container array (Fig. 1). Furthermore, a line source of emissions was placed at the ground level of the second street canyon. The line source system consisted of a gas emission source, which was connected to a 19-m long, closed-end, perforated pipe distributor with an internal diameter of 50 mm. The number of holes (14 holes) and their diameter (5 mm) were suitably selected to achieve uniform distribution of gas emission along the entire length of the street canyon (Fig. 2).

To test the performance of the photocatalytic coverings two scenarios were investigated. During the first scenario, the wall surfaces of the second consecutive street canyon were covered with TiO_2 -treated cementitious plates, while during the second scenario the wall surfaces of the same street canyon were covered with non-treated cementitious plates. During both scenarios, in-street canyon concentrations measurements of NO_x were taken from the same two locations, namely, at the mid cross-section at 15% of the buildings height H , one at each of the building walls (Fig. 3).

Results from the field site measurements are presented later in section 3.4, in conjunction with a comparison between numerical results obtained with MIMO and the actual field site measurements, for both scenarios.

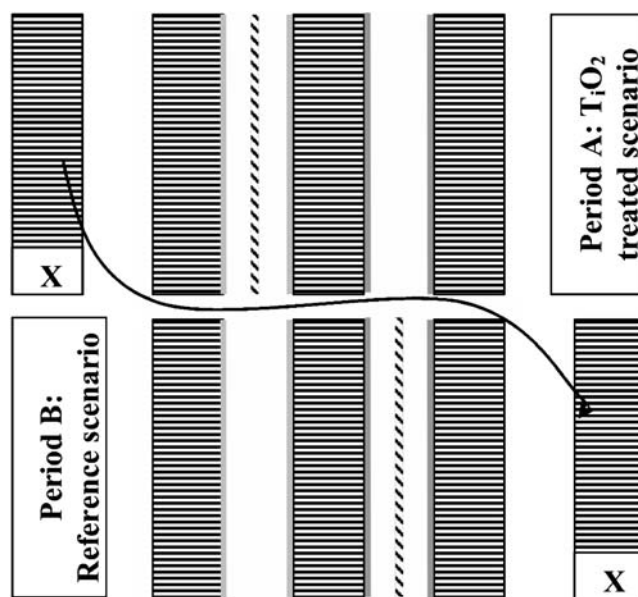


Fig. 3 The two scenarios investigated during the campaign

Table 1 Standard k - ε model constants including Prandtl and Schmidt numbers [21]

| C_μ | σ_κ | σ_ε | $C_{\varepsilon 1}$ | $C_{\varepsilon 2}$ | Pr_1 | Sc_1 |
|---------|-----------------|----------------------|---------------------|---------------------|--------|--------|
| 0.09 | 1.0 | 1.3 | 1.44 | 1.92 | 0.7 | 0.9 |

3 Numerical Modeling

Extensive numerical modeling was performed with the application of MIMO in an effort to assess the sensitivity of the flow field and the dispersion mechanism in the field site configuration and hence of the expected depollution effectiveness of the photocatalytic product, which was going to be tested.

3.1 The Microscale Model MIMO

The numerical model MIMO is a three-dimensional RANS CFD code for simulating microscale wind flow and dispersion of pollutants in built-up areas. It solves the Reynolds averaged conservation equations for mass, momentum and energy. In addition, transport equations for humidity, liquid water content and passive pollutants can be solved. A staggered grid arrangement is used and coordinate transformation is applied to allow non-equidistant mesh size in all three dimensions to achieve a high resolution near the ground and near obstacles [7]. The Reynolds stresses and turbulent fluxes of scalar quantities can be calculated by several linear and nonlinear

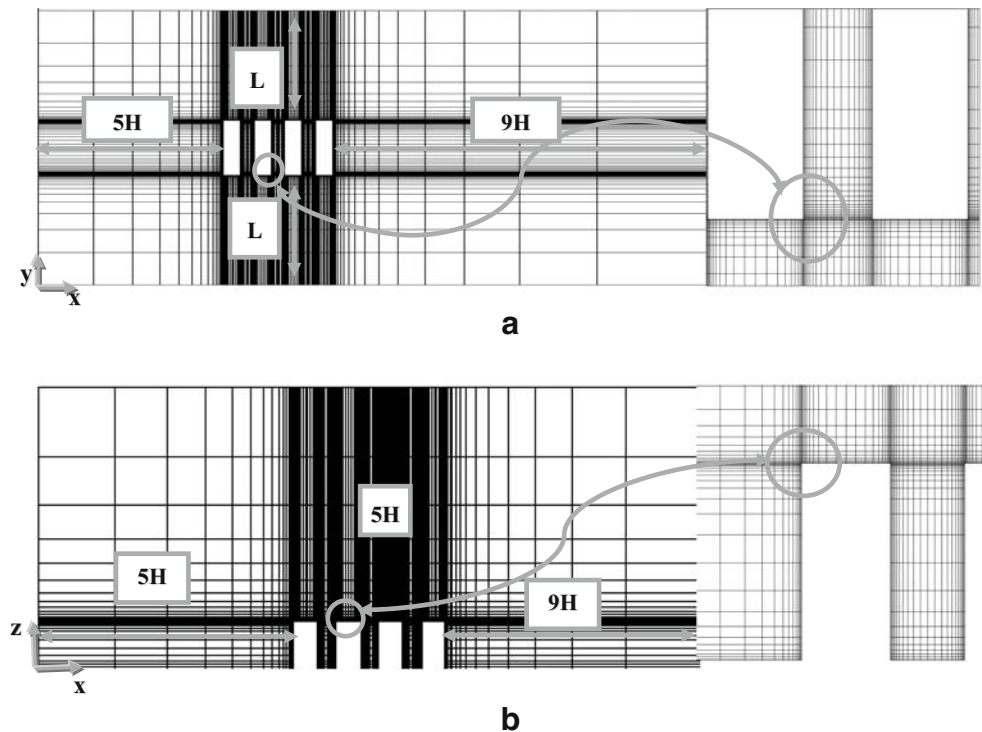
turbulence models [6]. For the needs of the present numerical studies the standard k - ε two-equation turbulence model by Jones and Launder in conjunction with the standard wall functions was utilised, because it is widely used and has been tested for various similar cases with very satisfactory results (Table 1).

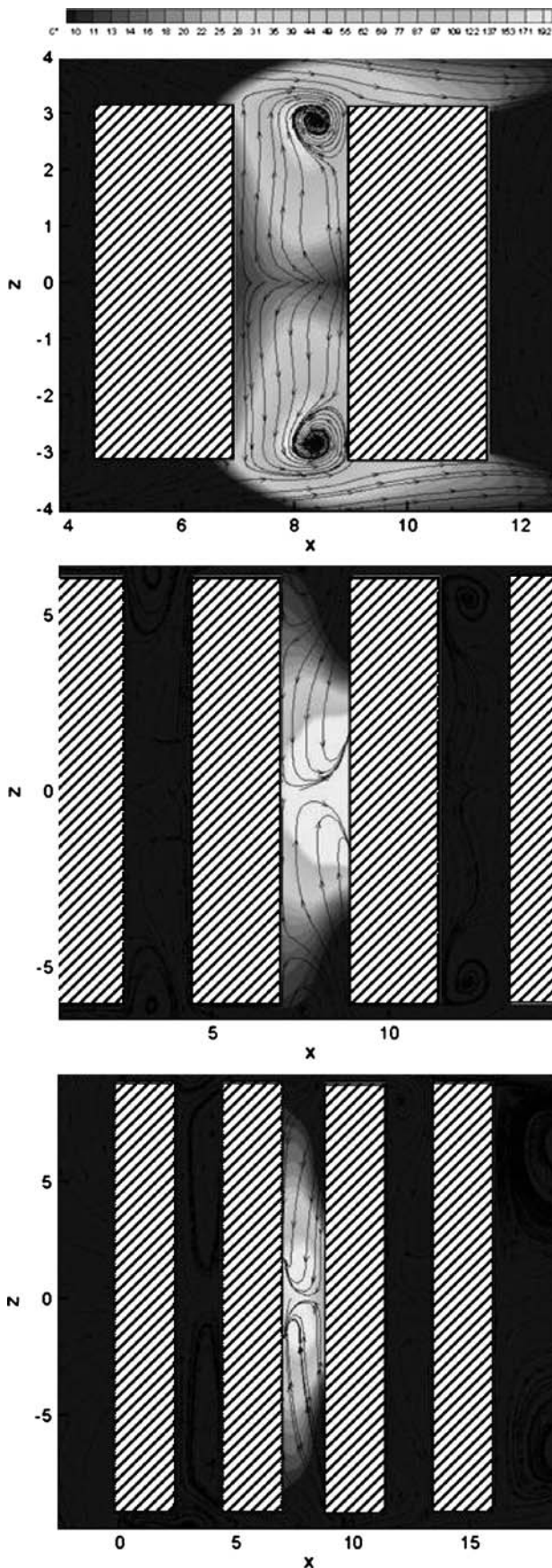
The governing equations are solved numerically on a staggered grid by using a finite volume discretization procedure. For the numerical treatment of advective transport there is an option between a 3D second-order total variation-diminishing (TVD) scheme [9] and a second-order flux-corrected transport (FCT) Adams Bashforth scheme (Wortmann et al., 1995) [22]. Both schemes are positive, transportive and conservative and they are characterised by low levels of numerical diffusion.

3.1.1 The Heating Module

A heating module was implemented into MIMO to be able to investigate the effects of thermal exchange between the street air and the buildings. This heating module can calculate the heat transfer through conduction, convection and radiation. Radiative transfer in the atmosphere is calculated with an efficient scheme based on the emissivity method for long-wave radiation and an implicit multilayer method for short-wave radiation [15]. The surface temperature over the ground is computed from the surface heat budget equation. The soil temperature is calculated by solving a one-dimensional heat conduction equation for the

Fig. 4 Computational domain and corresponding grid used in the street canyon length effect study (a) plan view and (b) top view





◀ **Fig. 5** Non-dimensional concentration fields in and around the second consecutive street canyon for the three cases at a height $Z=0.15H$, as computed by MIMO

soil. At lateral boundaries generalised radiation conditions are implemented. The nonlinear heat balance equation solved in MIMO heating module is written below:

$$R \downarrow_0 - R \uparrow_0 + S \downarrow_0 - S \uparrow_0 - Q_s - Q_o - L_o - Q_a = 0, \quad (1)$$

where R represents the long-wave radiative fluxes in and out, S represents the short-wave radiative fluxes in and out ($R_o \sim T_o^4$), Q_s is the heat flux to the ground (or wall), Q_a is the anthropogenic heat flux, Q_o is the sensible heat to the atmosphere and L_o is the latent heat to the atmosphere.

Regarding the transfer of heat from the street canyon walls to the air, the heat transfer coefficient is calculated via the following formula:

$$\alpha = \frac{|Q_f|}{(T_o - T_\infty)} = \frac{\rho c_p |u_* \theta_*|}{(T_o - T_\infty)} \quad (2)$$

where u_* is the friction velocity, θ_* is the surface layer temperature scale, ρ is the air density, c_p is the specific heat at constant pressure, T_o is the heated wall temperature and T_∞ is the temperature of the air close to the wall [13].

3.1.2 Photocatalytic Destruction Rate Module

For the needs of the PICADA project a simple, so-called “deposition” module was implemented into MIMO. This module was designed to approximate the removal of NO_x , which comes into contact with the treated street canyon walls, because of the photocatalytic action of the TiO_2 -based PICADA product. Through a series of extensive tests on laboratory scale, the NO_x destruction rate capacity of every individual sample that has been developed was quantified in terms of a specific “deposition” velocity, U_{dep} . It should be noted at this point, that this so-called “deposition” velocity, which is a material characteristic of the PICADA products, should not be confused with the commonly known deposition velocity used to describe physical phenomena such as wet and dry deposition. At any treated surface, for a given deposition velocity and for a given concentration calculated by the model at the first grid node near the wall, the deposition flux F_d is calculated via the following formula:

$$F_d = U_{dep} \times C_{wall\ average}, \quad (3)$$

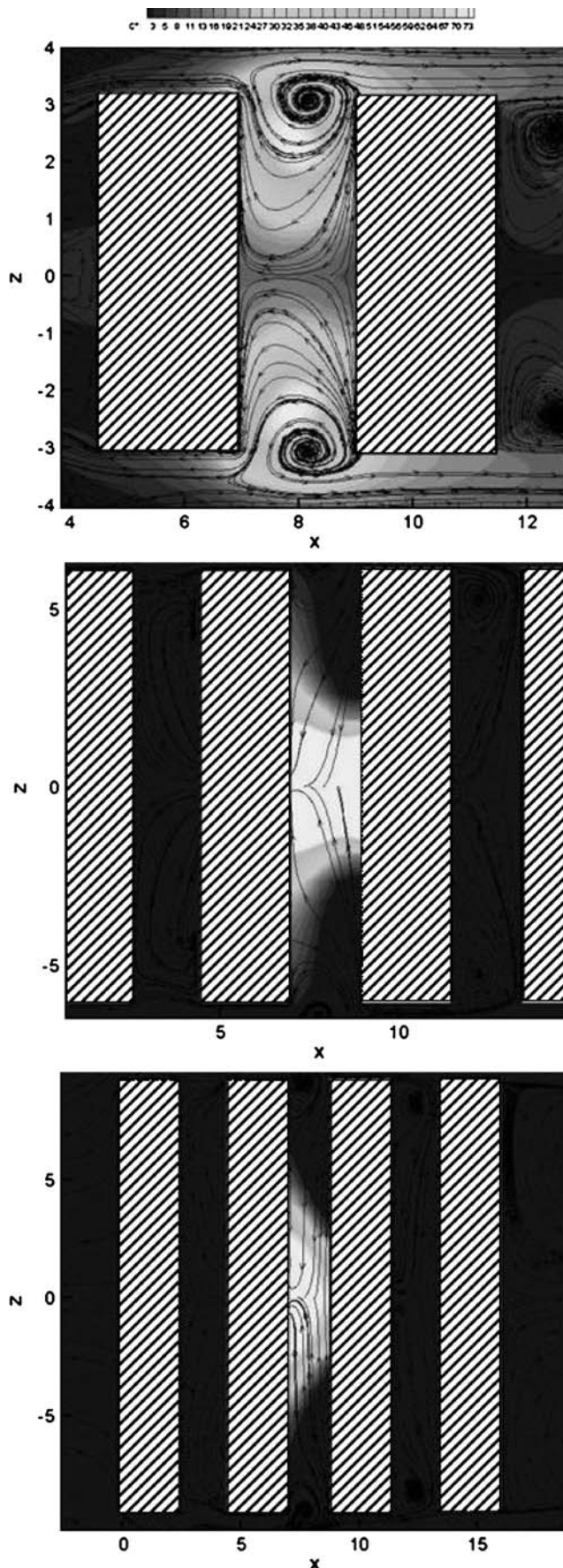


Fig. 6 Non-dimensional concentration fields in and around the second consecutive street canyon for the three cases at a height $Z=0.5H$, as computed by MIMO

where U_{dep} is the deposition velocity (m/s) and $C_{\text{wall average}}$ is the average concentration (kg/m^3) measured in the first node near the wall given by:

$$C_{\text{wall average}} = \frac{\sum_{i=1}^n \sum_{j=1}^m C_{ij}}{n \times m}, \quad (4)$$

where n and m are the number of nodes that define the treated surface along the i and j directions, respectively. Therefore, based on this deposition flux, for a known area of the treated wall it is possible to calculate the amount of pollutant mass that is removed because of the photocatalytic effect of the TiO_2 coverings. The percent of pollutant mass, which is removed at the treated walls, is then estimated as follows:

$$\text{NO}_x \text{ removed (\%)} = \frac{\dot{M}_{\text{NO}_x \text{ removed at wall}}}{\dot{M}_{\text{NO}_x \text{ emitted from source}}} \quad (5)$$

3.2 Street Canyon Length Effect Study

To determine the appropriate length of the field site street canyon configuration, a 3D numerical study was undertaken during which three cases with street canyons of different lengths were considered. In all cases investigated, the height of the street canyon buildings and the street width to street building ratio W/H was retained the same (0.4) and a line source of emissions was placed at the ground level of the second consecutive street canyon, extending along its entire length. In the first case, the canyon length was assumed to be slightly above 6 m ($L=6.096$ m; this is the length of one cargo container as those used in the field site), while in the second and third cases the street canyon length was set equal to that of two and three cargo containers, respectively (12.192 and 18.276 m).

3.2.1 Computational Domain and Grid Specifications

The computational domains were kept similar in all cases: the inlet of the domain was located at $5H$ upstream of the container arrays, the outlet at a distance of $9H$ downstream of the array, the top boundary at $5H$ above the roof level, whereas the lateral boundaries were placed at a distance L from the sides of the street canyon configuration (Fig. 4). Symmetry conditions were applied at the lateral boundaries, Dirichlet conditions at the top boundary and open conditions at the outlet boundary of the domain. The grid

Fig. 7 Non-dimensional concentration fields in and around the second consecutive street canyon for the three cases at a height $Z=H$ (roof level), as computed by MIMO

specifications were also kept the same in all cases that were investigated: the minimum cell size was chosen as 0.05 m with an expansion factor of 1.2, which resulted into a minimum y^+ value of ~ 30 .

3.2.2 Boundary Conditions

During all cases, the same boundary conditions were applied. At the inlet of the computational domain, the approaching flow direction was perpendicular to the street canyon axis, while the boundary layer characteristics were assumed in accordance with VDI 3783/Part 12 guidelines for flows over rough areas. The modelled approach flow boundary layer is described by the following logarithmic formula:

$$\frac{\bar{u}(z)}{u_*} = \frac{1}{\kappa} \ln \left(\frac{z - d_0}{z_0} \right), \tag{6}$$

where $\bar{u}(z)$ is the mean velocity at elevation z , z_0 is the surface roughness length, κ is von Karman's constant, d_0 is the displacement height and u_* is the friction velocity. In our case, the roughness length is 0.4 m, von Karman's constant is 0.4 and the friction velocity is 0.47 m/s. In MIMO, the approach flow boundary layer is modeled via the following logarithmic formula at the inlet of the computation domain:

$$\frac{\bar{u}(z)}{u_{ref}} = \left(\frac{z}{z_{ref}} \right)^\alpha \tag{7}$$

with $U_{ref}=5$ m/s at the surface layer height $z_{ref}=35$ m and a profile exponent $\alpha=0.24$. During this study all cases were treated as isothermal.

3.2.3 Results and Discussion

For the 3D cases that were investigated with MIMO, results were extracted at horizontal planes at the heights of $Z/H=0.15$, $Z/H=0.5$ and $Z/H=1.0$. As expected, the patterns are symmetrical with respect to the axis $Y=0$. In all three cases, the dispersion pattern of the pollutants is dominated by the coupling of vortices generated in the vertical and horizontal directions. Vortices generated in the horizontal direction act in the same way like the ones generated in the vertical direction that apparently dominate the flow fields in 2D street canyons in which only the u and w velocity components are important. In 3D cases, however, the component along the canyon axis is also important, as it dominates the

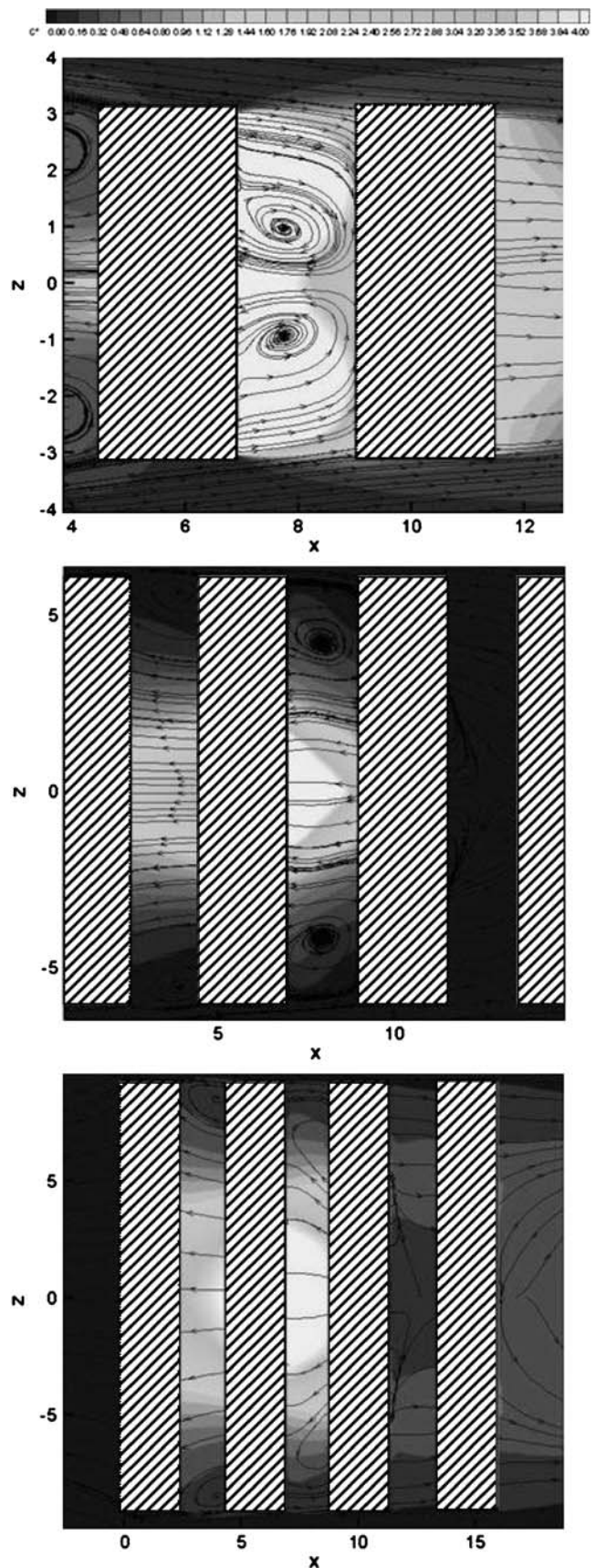
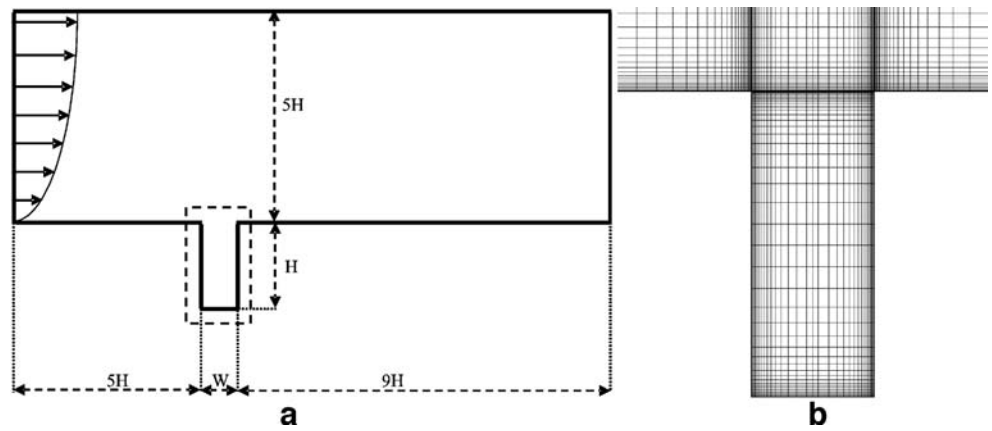


Fig. 8 (a) Computational domain and (b) grid details of the 2D cavity of aspect ratio 0.4



inward–outward mass flux between the centre and the sides of the street canyon. As a result, in the first case the vortices at the two sides of the street canyon drive pollutants in a region near there. On the other hand, the system of vortices that develops inside the street canyons in the other two cases results in the accumulation of the pollutants in a region near the vertical middle plane section of the street canyon. The highest concentrations of pollutants in the three cases under investigation are observed at the low levels of the third configuration.

The calculated concentrations are presented in their non-dimensional form:

$$C^* = CU_\delta H / (Q_s / L) \tag{8}$$

where C^* is the non-dimensional concentration, C is the calculated pollutant concentration, U_δ is the reference wind velocity, H is the height of the street canyon, Q_s is the mass flow of the pollutant emission and L is the characteristic length of the source. Figures 5, 6, and 7 show the dimension-

less concentration fields computed by MIMO for the three street canyon length cases, at three horizontal levels at heights of $Z=0.15H$, $Z=0.5H$ and $Z=H$ (roof level). The third configuration is the one that was chosen as the experimental street canyon configuration for the PICADA field experiment.

3.3 Heat Transfer Effect Study

In addition to the numerical study described above, several 2D simulations for the experimental aspect ratio of the field site street canyon configuration (0.4) with and without wall heating were performed, to investigate the effects of heat transfer between the heated building walls by solar radiation and the street canyon air on the flow and concentration fields and hence on the expected depollution efficiency of the photocatalytic coverings. The simulations were performed

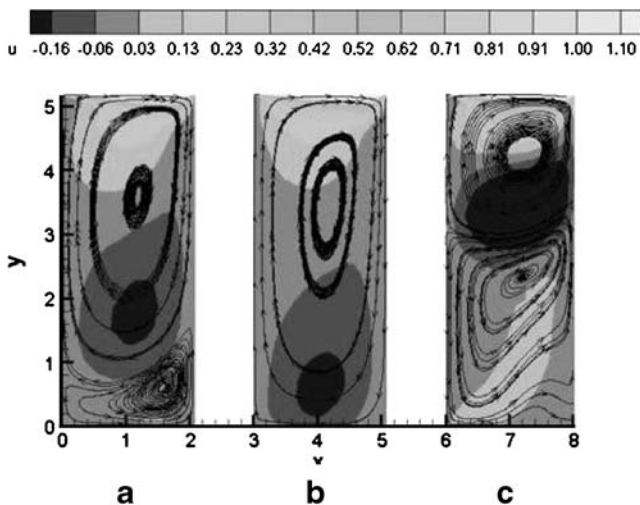


Fig. 9 U velocity field comparison for aspect ratio 0.4 as computed by MIMO for (a) the isothermal, (b) the leeward, and (c) the windward heated cases, respectively, for $\Delta T=15$ K

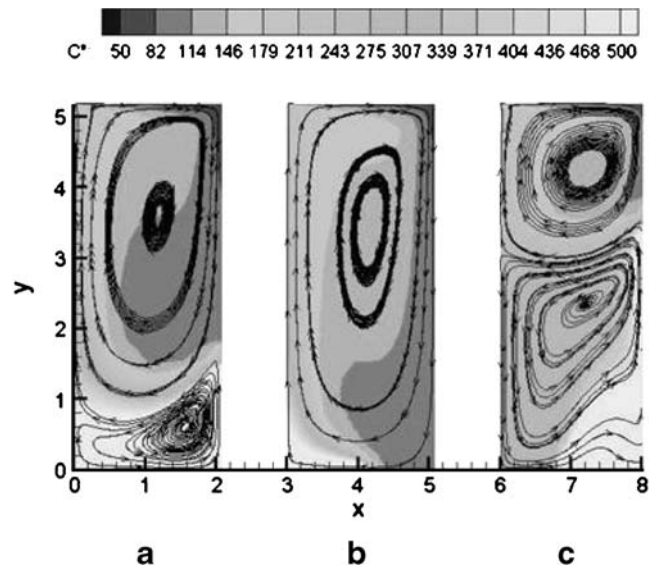


Fig. 10 Dimensionless concentration comparison for aspect ratio 0.4 as computed by MIMO for (a) the isothermal, (b) the leeward and (c) the windward heated cases, respectively, for $\Delta T=15$ K

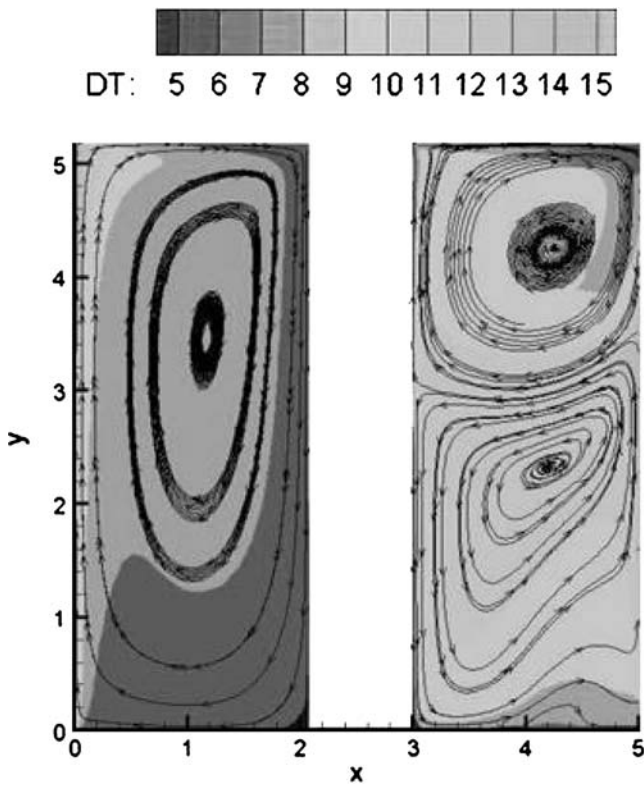


Fig. 11 Temperature difference between the heated walls and the street canyon air for (a) the leeward and (b) the windward heated cases respectively, for $\Delta T=15$ K

with two different deposition velocities, namely, (a) $U_{dep}=0.166$ cm/s and (b) $U_{dep}=0.5$ cm/s, which correspond to two different types of photocatalytic materials. The simulations were repeated for a negligible deposition velocity to analyze the reference situation (i.e., without the photocatalytic material).

3.3.1 Computational Domain and Grid Specifications

During all simulations the 2D street canyon was treated as a cavity with a height $H=5.182$ m, aspect ratio 0.4 and a resulting street canyon width $W=2.072$ m. The inlet of the domain was located at a distance $5H$ upstream, the outlet at

Table 2 Removal of NO_x at the treated street canyon walls for the two products for the three heating cases, respectively

| Heating case | NO_x removed (%) | |
|----------------------|--------------------------------------|------------------------------------|
| | Product 1 ($U_{dep}=0.166$ cm/s) | Product 2 ($U_{dep}=0.5$ cm/s) |
| Isothermal | 23.6 | 88.7 |
| Leeward wall heated | 11.1 | 41.8 |
| Windward wall heated | 27.0 | 94.8 |

a distance of $9H$ downstream and the top boundary at a height of $5H$ above the roof level of the cavity. The grid specifications were the same as in the 3D numerical study for the effect of the street canyon length described in the

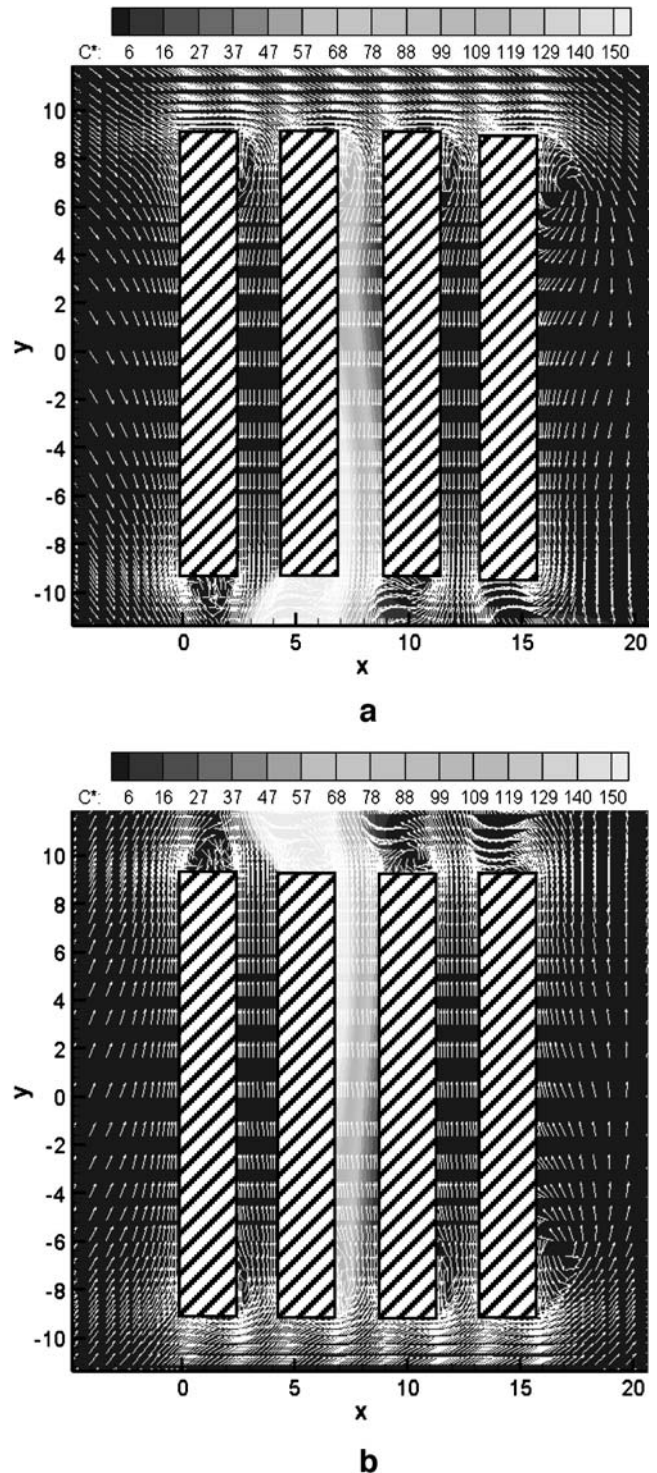


Fig. 12 Flow and concentration fields for approach flow direction for (a) 0° and (b) 270°

previous section: minimum cell size of 0.05 m with an expansion factor of 1.2 (Fig. 8). The boundary conditions at the faces of the domain were the same as in the ones described in section 3.2.1.

3.3.2 Boundary Conditions

As this was a 2D study and the street canyon was approximated as a cavity, the approaching wind direction was by definition perpendicular to the street canyon with an assumed inlet velocity of 5 m/s at a reference height of 35 m. Furthermore, in all cases the approach flow boundary layer was modelled in the same way as in the 3D numerical study for the effect of the street canyon length. The temperature difference (ΔT) between the heated wall (leeward or windward) and the ambient air was assumed to be 15 K.

3.3.3 Results and Discussion

From the results it is evident that for this 2D street canyon of aspect ratio 0.4, under isothermal conditions, two mechanically induced counter-rotating vortices form [1, 16, 21]. Moreover, when the leeward wall is heated, only one vortex forms by the combination of the two counter-rotating vortices, which appear in the no-heating case. On the other hand, when the windward wall is heated, two counter-rotating vortices appear as in the no-heating case. However, compared with the no-heating case, the intensity and vertical extent of the lower vortex increase and those of the upper vortex decrease because of the thermal upward

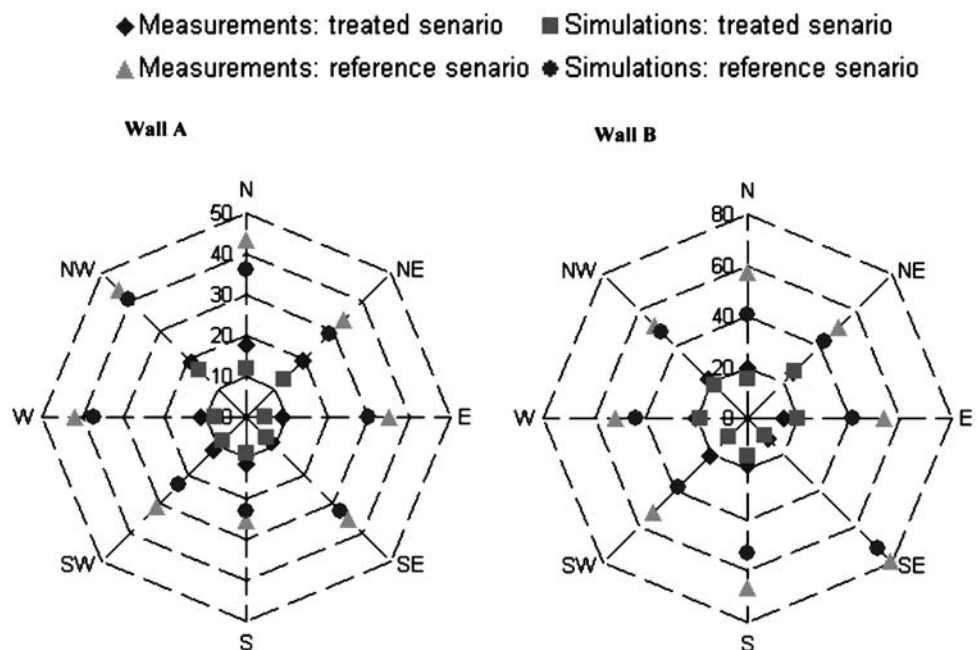
motion near the windward building [12]. Figures 9, 10, and 11 show the flow, the dimensionless concentration and the temperature field comparison between the isothermal, leeward- and windward-wall-heated cases, respectively.

As a result of these differences between the flow and concentration fields for the three cases that have been described above, the average predicted deposition flux and the corresponding depollution efficiency of the two photocatalytic products under investigation varies considerably between the three cases. The lowest deposition flux at the treated street canyon walls is observed when the leeward wall of the street canyon is heated, while the highest one is observed when the windward wall is heated (Table 2).

3.4 Approaching Wind Direction Effect Study

After the field site street canyon configuration design was finalised based on the results obtained from the numerical studies described in the previous section, an additional 3D numerical study was also undertaken to investigate the effect of the approaching wind direction on (a) the predicted flow and concentration fields in and around the street canyon configuration and (b) the expected depollution efficiency of the product, which was going to be tested (product 2 in Table 2). Furthermore, upon completion of the field experiment the numerical results would then be compared with the actual field site NO_x measurements on both walls of the street canyon. Simulations were initially performed for 16 different wind directions, ranging from 0° to 360° at steps of 22.5° using a deposition velocity

Fig. 13 Comparison between numerical results and field site measurements for mean NO_x concentrations (ppb) per wind sector for both walls and for both scenarios



$U_{\text{dep}}=0.5$ cm/s and they were then repeated for a negligible deposition velocity to analyse the reference scenario.

3.4.1 Computational Domain and Grid Specifications

During all simulations the same computational domain and grid specifications were used. Both the computational domain and the grid specifications were the same as the ones used in the third case under investigation during the 3D street canyon length effect study described in section 3.2.1, as this was the configuration that had been chosen for the experiment. In the same sense, a line source of emissions was placed at the ground level of the second consecutive street canyon extending along its entire length.

3.4.2 Boundary Conditions

During all numerical simulations, the modeled approach flow boundary layer characteristics were the same as the ones described in section 3.2.2. However, in this case, 16 different approaching wind directions were used with an assumed inlet reference velocity $U_{\text{ref}}=5$ m/s, defined at a reference height of 35 m at a distance of $5H$ upstream of the container array. Furthermore, during this study, input from in situ background NO_x concentration measurements and from gas emissions measurements for the line source were used.

3.4.3 Results and Discussion

Model results for NO_x concentrations were extracted at the exact same locations as the measuring points in the field site, for both scenarios. These results were then interpolated to cover the whole range of wind directions from 0° to 360° with a step of 1° . Furthermore, by assuming a simple scaling of the numerically calculated concentrations with wind speed and emissions of $1/U$ [10, 11], these interpolated NO_x concentration results on both walls and for both scenarios were used to calculate NO_x concentrations for a range of speeds from 1 m/s up to 10 m/s at a step of 1 m/s, for all wind directions. The results were then correlated with the corresponding field site NO_x measurements based on the wind direction and wind speed for both scenarios, for the entire duration of the field campaign and comparison between the two was made.

The numerical results clearly indicate that maximum concentrations inside the field site street canyon configuration are observed when the approaching wind direction is perpendicular to the street canyon axis. Furthermore, for approaching wind directions close to the perpendicular with respect to the street canyon axis, pollutants tend to concentrate at a region near the middle cross-section of the street canyon, with the exchange of air being dominated mainly by vertical pollutant transport with only a small

portion leaving the canyon from its side exits. However, even small deviations from the perpendicular direction lead to a significant street-parallel velocity component with a corresponding transport of pollutants to the canyon edge [5]. As a result, the flushing via one canyon side is considerably enforced with a corresponding reduction of the mass transported out of the street canyon via the roof top (Fig. 12, [3]).

Moreover, the comparison between numerical results with MIMO and field site measurements shows that MIMO results are in a very good agreement with the field measurements, with only a relatively small underestimation of the NO_x concentrations for both scenarios by MIMO. Furthermore, both the numerical results and the field site measurements prove that the TiO_2 -based photocatalytic coverings are indeed capable of removing NO_x from the urban environment. Both the numerical results and the actual field measurements, for both walls and for both scenarios were classified according to the approaching wind speed and direction. Both the measurements and the numerical results indicate a reduction in the concentration of NO_x on both walls, which ranges from $\sim 41\%$ up to $\sim 82\%$ for Wall A and from $\sim 35\%$ up to $\sim 75\%$ for Wall B, with an average reduction of the NO_x concentration for both walls as a result of the use of the photocatalytic product between 50 and 60% (Fig. 13).

4 Conclusions

Overall in conclusion, the comparison between numerical simulations and experimental results shows very good agreement between the two and proves that MIMO is capable of accurately describing the impact of photocatalytic TiO_2 coverings on the NO_x levels in an urban street canyon. Furthermore, both the numerical results and the field site measurements have shown that the reduction of NO_x concentrations inside the experimental field site configurations as a result of the use of the photocatalytic coverings is significant.

The results from the various numerical studies that were performed indicate that the flow field and the corresponding dispersion mechanism in an urban street canyon are indeed very sensitive and can be affected by many factors. Depending on the length of the street canyon, pollution will accumulate to different positions because of the different systems of vortices that develop on the horizontal direction. The results have shown that longer streets are ventilated less efficiently than short ones, and as a result in real urban environments we should expect lower air quality in long streets.

Furthermore, numerical results indicate that the flow field inside a deep street canyon can be influenced by thermal exchange between the heated walls and the street canyon air.

Yet, in this specific experiment thermal effects seem to affect only slightly the overall depollution efficiency of the photocatalytic products.

Also, numerical simulations made specifically for the experimental field site, proved that the dispersion mechanism in a street is particularly sensitive to the approaching wind direction. Even small deviations of the approaching direction perpendicular to the street canyon axis can enforce the transport of pollution out of the canyon and improve its ventilation characteristics.

Acknowledgements The authors gratefully acknowledge funding from the PICADA project (Contract No. GRD1-2001-40449) within GROWTH Measurements & Testing Infrastructures, EC's 5th Framework Programme.

References

- Baik, J.-J., & Kim, J.-J. (1998). A numerical study of flow and pollutant dispersion characteristics in urban street canyons. *Journal of applied meteorology*, *38*, 1576–1589.
- Baik, J.-J., Park, R.-S., Chun, H.-Y., & Kim, J.-J. (1999). A laboratory model of urban street-canyon flows. *Journal of applied meteorology*, *39*, 1592–1600.
- Barmpas, P., Leiti, B., Moussiopoulos, N., & Schatzmann, M. (2005). Physical modeling of flow and dispersion in and around an idealised street canyon – replicating the PICADA field experiment in a boundary layer wind tunnel. Proceedings of the 5th International Conference on Urban Air Quality, Valencia, Spain, 29–31 March.
- Berkowicz, R. (1998). *Street scale models in urban air pollution*. Kluwer Academic, 223–252.
- Crowther, J., & Hassan, A. (2002). Three-dimensional numerical simulation of air pollutant dispersion in street canyons. *Water, air, and soil pollution: Focus* *2*, 279–295.
- Ehrhard, J. (1999). Untersuchung linearer und nightlinearer Wirbelviskositätsmodelle zur Berechnung turbulenter Stromungen um Gebäude. *Dissertation*, University of Karlsruhe, Department of Applied Thermodynamics.
- Ehrhard, J., Khatib, I. A., Winkler, C., Kunz, R., Moussiopoulos, N., & Ernst, G. (2000). The microscale model MIMO: development and assessment. *Journal of Wind Engineering and Industrial Aerodynamics*, *85*, 163–176.
- Fujishima, A. (2002). Recent trends in photocatalytic research and in the industry. *Science and technology in Japan*, *83*, 27–32.
- Harten, A. (1986). On a large time-step high resolution scheme. *Mathematics and computation*, *46*, 379–399.
- Kastner-Klein, P., Berkowicz, R., & Fedorovich, E. (2001). Evaluation of scaling concepts for traffic-produced turbulence based on laboratory and full-scale concentration measurements in street canyons. In: *Proceedings of the Third International Conference on Urban Air Quality* (19–23). March, Loutraki, Greece.
- Ketzel, M., Berkowicz, R., & Lohmeyer, A. (2000). Comparison of numerical street dispersion models with results from wind tunnel and field measurements. *Environmental monitoring and assessment*, *65*, 367–370.
- Kim, J. J., & Baik, J. J. (1999). A numerical study of thermal effects on flow and pollutants dispersion in urban street canyons. *Journal of applied meteorology*, *38*, 1249–1261.
- Kunz, R. (2001). Mathematische Modellierung des atmosphärischen Stofftransports und des Mikroklimas in bebauten Gebieten. VDI Verlag, Reihe 15, Nr. 236.
- Louka, P., Vachon, G., Sini, J. F., Mestayer, P. G., & Rosant, J.-M. (2001). Thermal effects on the airflow in a street canyon – Nantes '99 experimental results and model simulations. *Water, air and soil pollution: Focus*, *2*, 351–364.
- Moussiopoulos N. (1987). An efficient scheme to calculate radiative transfer in mesoscale models. *Environmental software*, *2*, 172–191.
- Moussiopoulos, N., Ossanlis, I., & Barmpas, P. (2005). A study of heat transfer effects on air pollution dispersion in street canyons by numerical simulations. *International journal of environment and pollution*, *25*, 1/2/3/4.
- Noguchi, H. (2002). Hybrid technology for environmental purifications using TiO₂ photocatalyst. *Science and technology in Japan*, *83*, 41–44.
- Oke, T. R. (1988). Street design and urban canopy layer climate. *Energy building*, *11*, 103–113.
- Ossanlis, I., Barmpas, Ph., & Moussiopoulos, N. (2004). The effect of street canyon length on the street scale flow field and air quality: a numerical study. Proceedings of 27th NATO/CCMS International Technical Meeting on Air Pollution Modelling and its Application, Canada, 25–29 October.
- Sang, J. J., & Malcom, J. A. (2001). Application of the k-ε turbulence model to the high Reynolds number skimming flow field of an urban street canyon. *Atmospheric environment*, *36*, 1137–1145.
- Sini, J. F., Anquentin, S., & Mestayer, P. G. (1996). Pollutant dispersion and thermal effects in urban street canyons. *Atmospheric environment*, *30*(15), 2659–2677.
- Wortmann-Vierthaler, M., & Moussiopoulos, N. (1995). Numerical tests of a refined flux corrected transport advection scheme. *Environmental software*, *10*, 157–176.

Nicolas Moussiopoulos is a Professor at the Department of Mechanical Engineering of the Aristotle University of Thessaloniki, Greece, and the Head of the Laboratory of Heat Transfer and Environmental Engineering. He is also an Honorary Professor at the School of Mechanical Engineering of the Universität Karlsruhe (since 1996) and a member of the German Academy of Natural Scientists Leopoldina (since 2002). In 1990 he received the well-known Heinrich Hertz Award. His research work is in the areas of energy systems and environmental engineering. He has been involved in several large EC projects and has contributed to several major environmental impact assessment studies. Nicolas Moussiopoulos has about 250 scientific publications, including more than 60 papers in peer-reviewed journals and 12 books.